Precise Measurement of the DIS Cross Section at Low Q^2 and Phenomenological Fits

Alexey Petrukhin

DESY
Notkestrasse 85, 22607 Hamburg, Germany
ITEP
Bolshaja Cheremushkinskaja 25, 117218 Moscow, Russia

Precise measurements of the DIS cross section at low Q^2 by the H1 Collaboration are summarized. This measurements are performed in the region of low squared four-momentum transfers, $0.2\,\mathrm{GeV}^2 \leq Q^2 \leq 12\,\mathrm{GeV}^2$, and low Bjorken x, $5{\cdot}10^{-6} \leq x \leq 0.02$. The data are compared to the different phenomenological models.

1 Introduction

At low Q^2 the DIS double-differential cross section in its reduced form can be expressed as:

$$\frac{d^2\sigma}{dx\,dQ^2} \cdot \frac{Q^4 x}{2\pi\alpha^2 Y_+} = \sigma_r = F_2(x,Q^2) - \frac{y^2}{Y_+} \cdot F_L(x,Q^2), \tag{1}$$

where Q^2 is the squared four-momentum transfer and x is the Bjorken scaling variable, $Y_+ = 1 + (1-y)^2$. The inelasticity $y = Q^2/sx$ is a fraction of the lepton's energy loss and s denotes the squared center of mass energy of the lepton-nucleon system. The double-differential cross section is governed by two independent proton structure functions, F_2 and F_L. For low y the contribution of F_L is supressed due to the kinematic factor y^2/Y_+. Therefore the measurement of σ_r at low y determines F_2 with a small correction for F_L.

2 Measurements of the DIS cross section

The data used in the recent analysis were taken by the H1 detector during special running periods with open triggers for inclusive DIS events. In order to access low values of Q^2 around 1 GeV^2 the interaction vertex for short period of H1 2000 data taking was shifted by approximately 70 cm along the proton beam direction. This data sample is also used for accessing larger values of x with Initial State Radiation (ISR) events. Data collected by the H1 collaboration in 1999 with a nominal position of the interaction vertex are used for measurements in the high y region. These data are combined with H1 data taken in 1995-1997. The 1997 data were corrected globally by +3.4% due to better understanding of the luminosity tagger acceptance.

The kinematic reconstruction by H1 is done with two methods. The sigma method [2] has been used for medium and low y and the electron method was prefered at highest y due to a better y resolution in this region. The H1 measurements of the DIS cross section at low Q^2 are shown in Figure 1(Left).

The new H1-9900 results extend the measured kinematic range towards low Q^2 and high x values by using ISR events. There is a good agreement in regions of overlap between new and previously published H1 data taking into account H1-95 normalisation uncertainty.

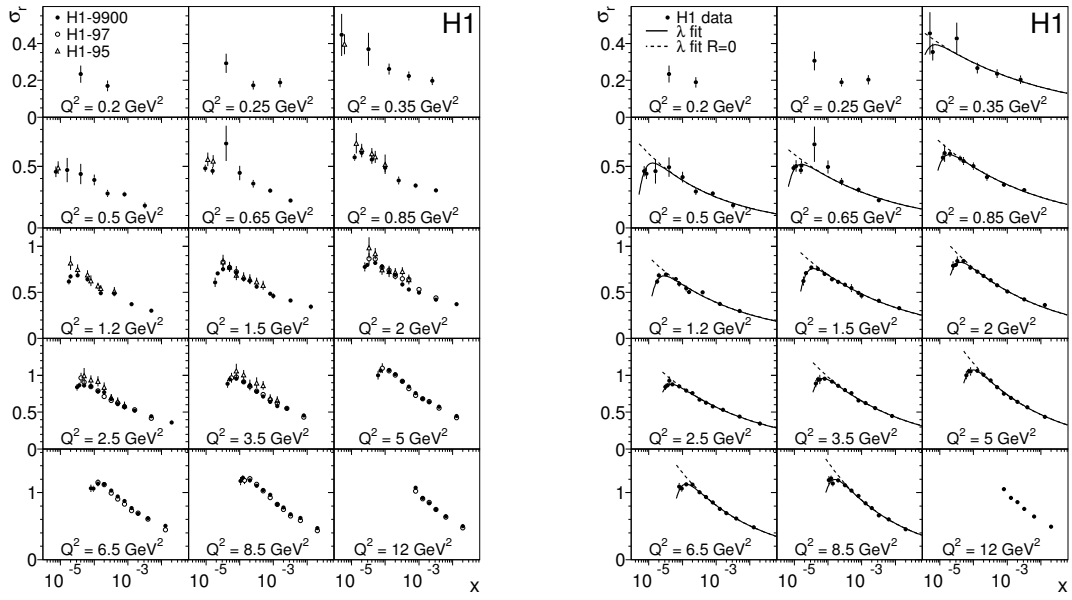

Figure 1: Reduced cross section σ_r. Left: Closed circles: combined 1999-2000 data; Triangles: data with a shifted interaction vertex taken in 1995 [3]; Open circles: data taken in 1997 [4]. Right: The combined low Q^2 H1 data, as a function of x compare to the λ fit result (solid line) and to a λ parameterisation with the same values of $c(Q^2)$ and $\lambda(Q^2)$ but $R = F_L/(F_2 - F_L) = 0$ (dashed line). The errors represent the statistical and systematic uncertainties added in quadrature.

3 Combined reduced cross section

A global combination of H1 1995-2000 data is performed following the prescription introduced in [5] taking into account bin-to-bin correlated systematic uncertainties. According to this procedure the combination of all data provides a single data set in the range $0.2\,\mathrm{GeV}^2 \leq Q^2 \leq 12\,\mathrm{GeV}^2$, and Bjorken x, $5 \cdot 10^{-6} \leq x \leq 0.02$. Systematic errors assumed to be uncorrelated between the different data sets. Good agreement between H1 data is observed with a $\chi^2/n_{\mathrm{dof}} = 86/125$. The precision of the combined data set is high, up to 1.5% in the central Q^2, x region of the measurement. The combined reduced cross section at low Q^2 measured by H1 is presented in Figure 1(Right).

The rise of the structure function F_2 towards low x has previously been described by a power law in x, $F_2 = c(Q^2)x^{-\lambda(Q^2)}$, where the exponent λ increases approximately logarithmically with $\ln Q^2$ for $Q^2 \gtrsim 2\,\mathrm{GeV}^2$ [6]. This simple parameterisation has been shown to model the *ep* data well for $x < 0.01$. This idea is extended to fit the reduced cross section σ_r in different Q^2 bins in order to simultaneously extract the $\lambda(Q^2)$, $c(Q^2)$ and to estimate the longitudinal structure function F_L. The results of λ fit in different Q^2 bins are shown in Figure 1(Right). This simple parameterisation describes combined H1 data well.

4 Model comparison

The combined H1 data are also analysed in the context of the fractal model [7] and two versions of the colour dipole model [8,9], which may be applied to describe the transition region from photoproduction to deep inelastic scattering.

In the fractal model, the proton structure function F_2 is parameterised using five parameters Q_0 and D_0 to D_3 as

$$F_2(Q^2,x) = D_0 Q_0^2 \left(1+\frac{Q_0^2}{Q^2}\right)^{1-D_2} \frac{x^{-D_2+1}}{1+D_3-D_1\ln x} \left(x^{-D_1 \ln\left[1+\frac{Q^2}{Q_0^2}\right]} \left(1+\frac{Q^2}{Q_0^2}\right)^{D_3+1} - 1 \right) . \tag{2}$$

The parameters of this model are determined with a fit to the cross section data, except for the parameter D_2, which governs the structure function behaviour for the photoproduction regime and is fixed to $D_2 = 1.08$. The fractal model does not provide predictions for F_L. The same prescription is followed as for the λ fit described in the previous section taking the F_L contribution to be proportional to F_2. The values of F_L are found to be consistent with the λ fit. This agreement with the λ fit may be attributed to the structure function F_2 having a power law-like x dependence. The fractal fit describes the data well with $\chi^2/n_{\rm dof} = 155.3/(149-5)$.

The colour dipole model fits are three parameter fits which assume γ^*p scattering via γ^* splitting into dipole which scatters off the proton. In the GBW (Golec-Biernat and Wusthoff) model the dipole-proton cross section $\hat{\sigma}$ is given by

$$\hat{\sigma}(x,r) = \sigma_0 \left\{ 1 - \exp\left[-r^2 / \left(4 r_0^2(x) \right) \right] \right\} , \tag{3}$$

where r corresponds to the transverse separation between the quark and the antiquark, and r_0^2 is an x dependent scale parameter, assumed to have the form

$$r_0^2(x) \sim (x/x_0)^{\lambda} . \tag{4}$$

This model provides predictions for F_2 and F_L in terms of three parameters, σ_0, x_0 and λ. For $r \gg r_0$ it also predicts a saturation with a constant $\hat{\sigma} \simeq \sigma_0$ at $x = x_s$. The fit to the reduced cross section with the dipole model of GBW yields a $\chi^2/n_{\rm dof} = 183.1/(149-3)$, which is a bit worse than that for the fractal model. Another colour dipole model is IIM (Iancu, Itacura and Munier) fit. It uses a different model of the the dipole-proton cross section $\hat{\sigma}$ and yields a better $\chi^2/n_{\rm dof} = 178.2/(149-3)$.

Figure 2 shows that in general fractal and dipole models describe data well in most of the phase space. However a steeper rise of F_2 at low x from fractal fit as comared to dipole fits is observed.

To trace the origin of the χ^2 differences between the models, predictions for the structure functions F_2 and F_L are compared individually. As an example, Figure 3 shows the comparison between the three models for the bin $Q^2 = 1.2$ GeV^2.

The structure functions F_2 agree rather well for the models considered for $x > x_{\rm s}$, where $x_{\rm s}$ corresponds to the saturation radius of the GBW dipole model at the chosen Q^2 value. However, for $x < x_{\rm s}$ the dipole models show a softer F_2 dependence on x. This holds in particular for the IIM dipole model. The main difference between the models is in the structure function F_L. As shown in Figure 3, the predictions of the dipole models are nearly half of the result for F_L obtained with the fractal model analysis.

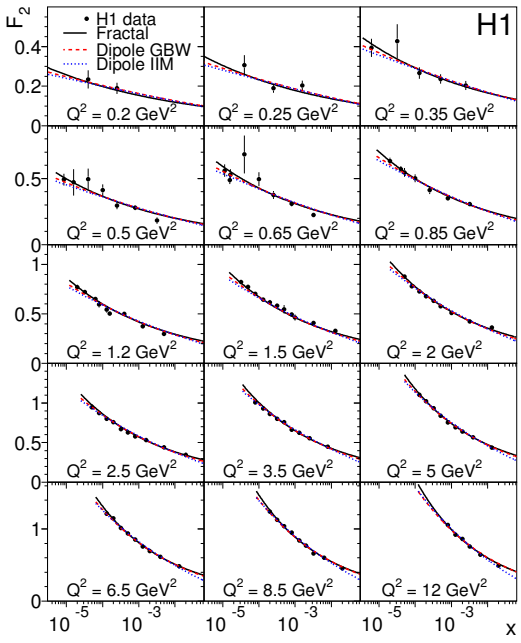

Figure 2: Structure function F_2, from the combined low Q^2 H1 data for $y < 0.6$, as a function of x compared to the fractal, the dipole GBW and the dipole IIM fit results. The errors represent the statistical and systematic uncertainties added in quadrature.

To quantify the influence of the structure function F_L another fit to the reduced cross section data is performed, in which the F_L prediction of the dipole model is scaled with an additional free parameter B_L

$$F_L(x, Q^2) = F_L^{\text{dipole}}(x, Q^2)\,(1 + B_L)\ . \tag{5}$$

With B_L as a formal free parameter the GBW fit returns $B_L = 0.54 \pm 0.15$. The fit for the IIM model does not yield a significant change for the F_L prediction: $B_L = 0.17 \pm 0.14$ in agreement with the observation that the IIM model with $B_L = 0$ already gave a better description of the data as compared to GBW.

5 Summary

The inclusive cross section measurements presented here extend the kinematic region covered by H1 at low Q^2 and high x. The achieved precision of the combined 1995-2000 DIS cross section data is up to the level of 1.5%. For the region $Q^2 \simeq 1\,\text{GeV}^2$, the data as presented here are the most precise result of the H1 Collaboration. The transition region from non-perturbative to deep inelastic behaviour is generally well described by the fractal and dipole colour models.

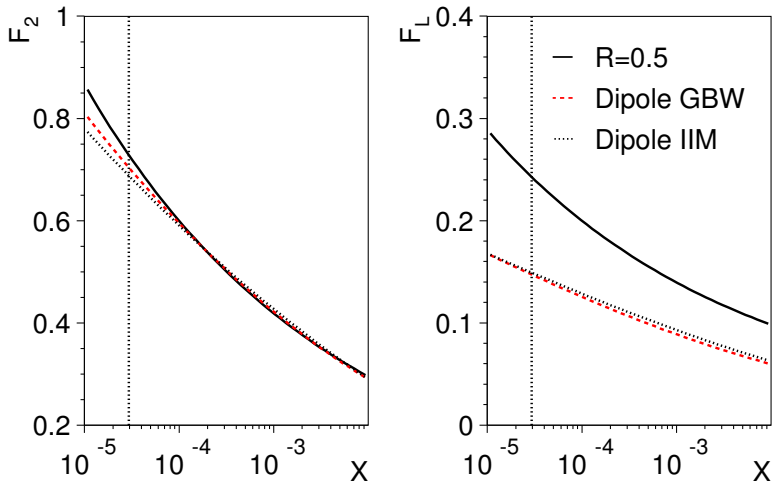

Figure 3: Comparison of the structure functions F_2 (left) and F_L (right) for $Q^2 = 1.2$ GeV^2 as a function of Bjorken x, for the fractal fit with $R = 0.5$ (solid line), and the predictions of the dipole models, GBW (dashed line) and IIM (dotted line), resulting from the fits to the H1 cross section data. The vertical line indicates the value of $x = x_s$ for which the GBW dipole model saturation radius is reached.

References

[1] Slides:
`http://indico.cern.ch/contributionDisplay.py?contribId=54&sessionId=0&confId=53294`

[2] U. Bassler, and G. Bernardi, Nucl. Instrum. Meth. **A361** 197 (1995).

[3] C. Adloff *et al.*, Nucl. Phys. **B497**, 3 (1997).

[4] C. Adloff *et al.*, Eur. Phys. J. **C21**, 33 (2001).

[5] A. Glazov, AIP Conf. Proc. **792** 237 (2005)

[6] C. Adloff *et al.*, Phys. Lett. **B487**, 183 (2001).

[7] T. Lastovicka, Eur. Phys. J. **C24**, 529 (2002).

[8] K. Golec-Biernat and M. Wusthoff, Phys. Rev. **D59**, 014017 (1999).

[9] E. Iancu, K. Itacura and S. Munier, Phys. Lett. **B590**, 199 (2004).